Electronic Supplementary Information

Aspartic Acid Based Metal–Organic Frameworks with Dual Function of NADH Peroxidase and Glycerol Dehydrogenase-Mimicking activities

Shuli Liu, Xiaoling Wu, Jun Xiong, Xin Yuan, Min-Hua Zong, Wen-Yong Lou**

Lab of Applied Biocatalysis, School of Food Science and Engineering, South China University of Technology, Guangzhou 510641, China.

*Corresponding author: Prof. W.-Y. Lou, E-mail: wylou@scut.edu.cn; Tel/Fax: +86-20-22236669; Dr. X.-L. Wu, E-mail: wuxl18@scut.edu.cn

KEYWORDS. Amino acid based metal-organic frameworks, Enzyme mimics, Cofactor regeneration, Glycerol dehydrogenase mimicking activity, 1,3-Dihydroxyacetone

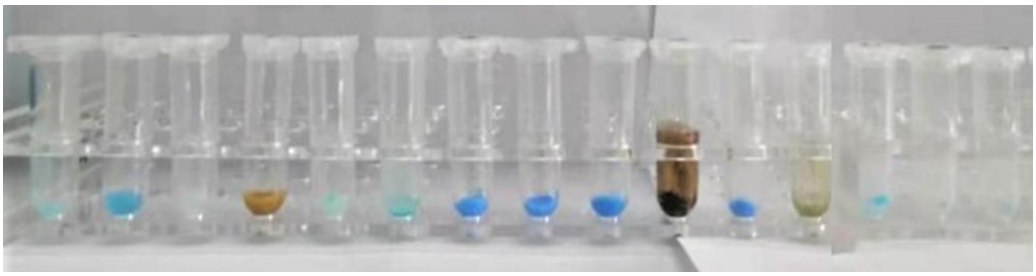

Figure S1. Photograph of MOF precipitates prepared from reaction of Cu^{2+} and different ligands at 60 ℃ for 20 hours. (from left to right, the ligands are OA, L-Ala, MA, AMA, TA, SA, L-Asp, D-Asp, DL-Asp, MSA, DASA, HAsp, GA, L-Glu and MAsp, respectively).

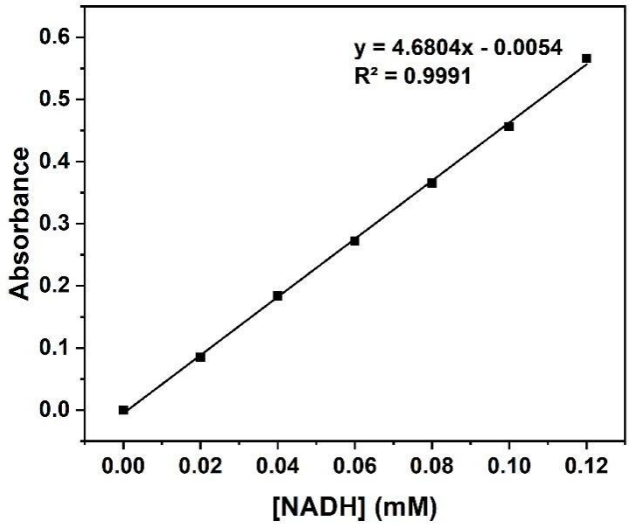

Figure S2. Standard curve of NADH.

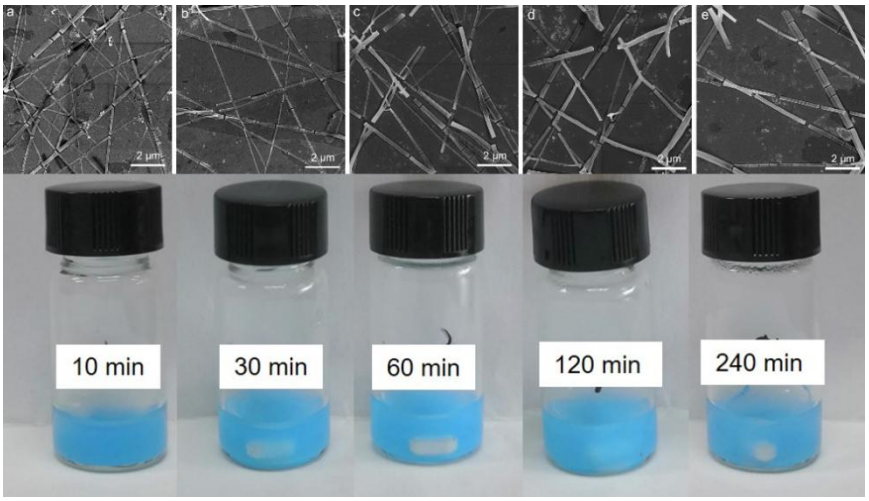

Figure S3. SEM images of CuAsp prepared for (a) 10 min, (b) 30 min, (c) 60min, (d) 120 min and (e) 240 min at room temperature and photographs of the mixture after reaction.

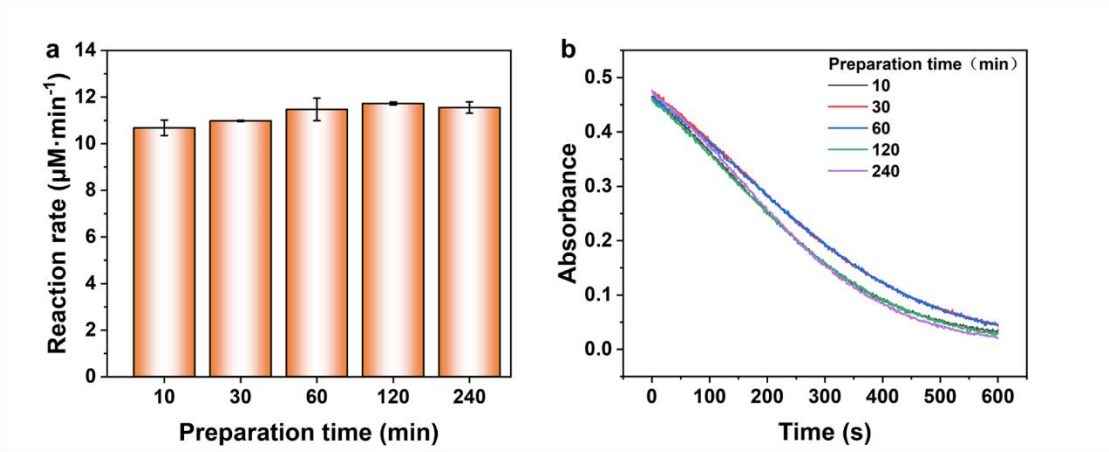

Figure S4. (a) NADH oxidation reaction rates catalyzed by CuAsp prepared for 10 min, 30 min, 60min, 120 min and 240 min and (b) the corresponding time-dependent absorbance changes at 340 nm.

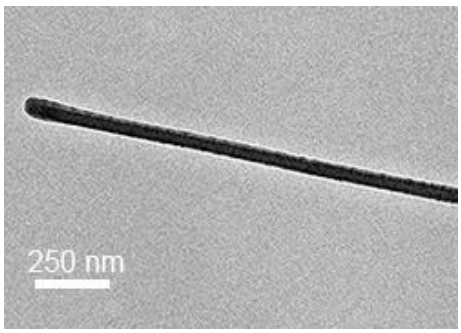

Figure S5. TEM image of CuAsp.

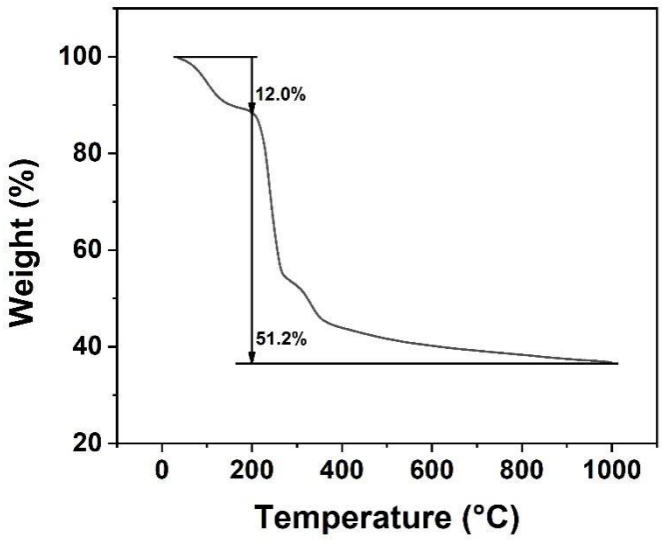

Figure S6. Thermogravimetric (TG) curve of CuAsp.

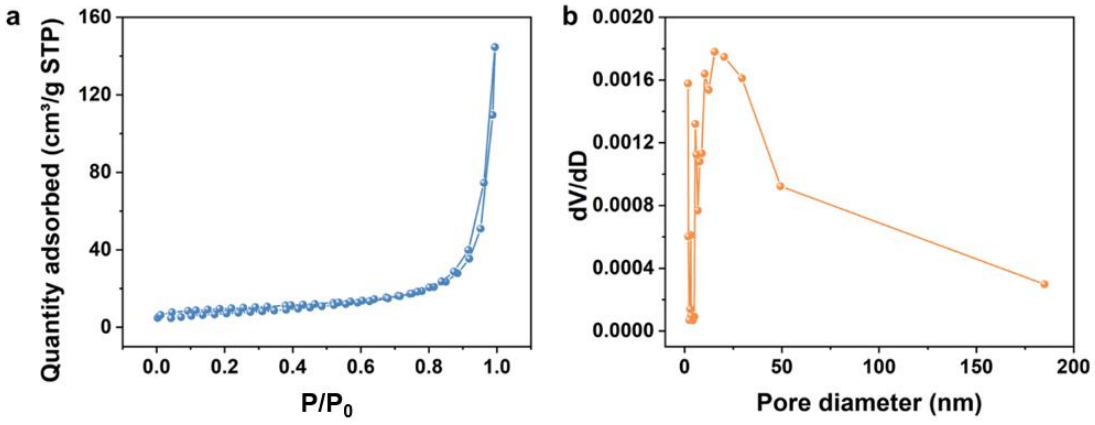

Figure S7. (a) N_2 adsorption-desorption isotherms and (b) pore size distribution curve of CuAsp.

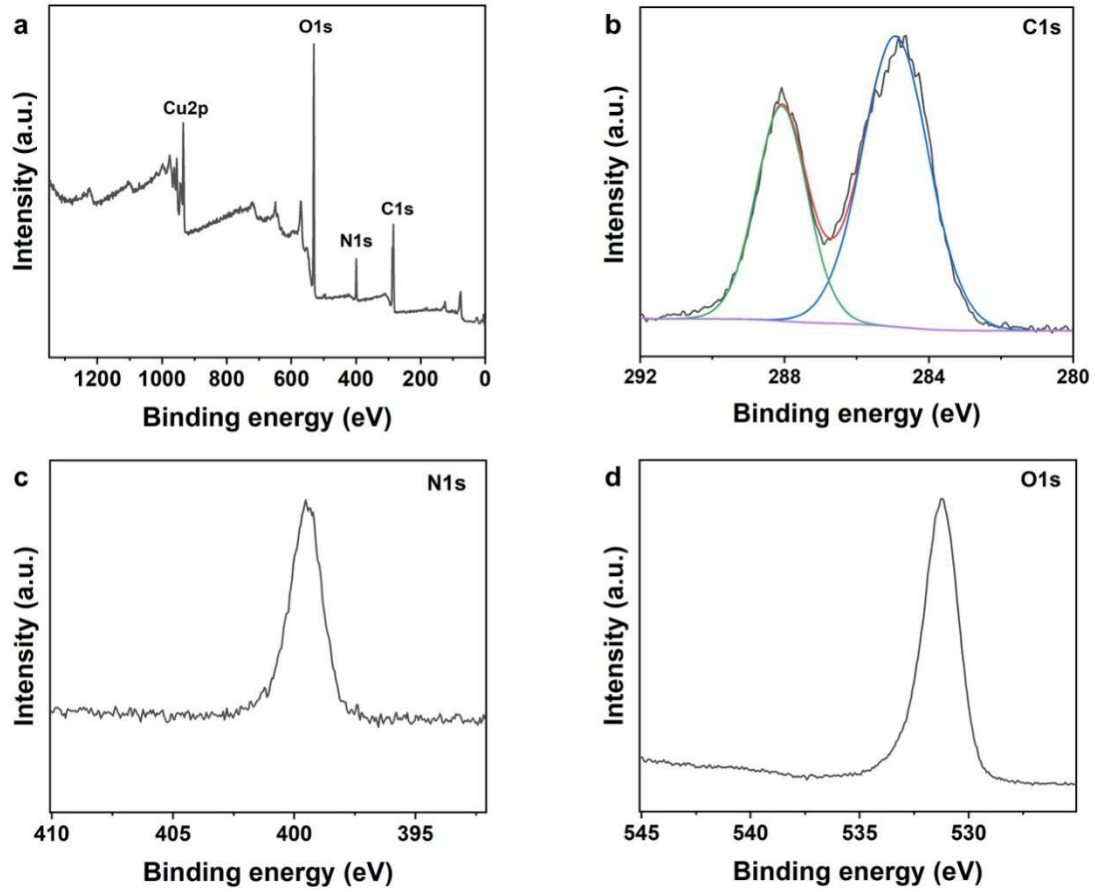

Figure S8. XPS spectra of CuAsp: (a) full scan; (b) C 1s; (c) N 1s; (d) O 1s.

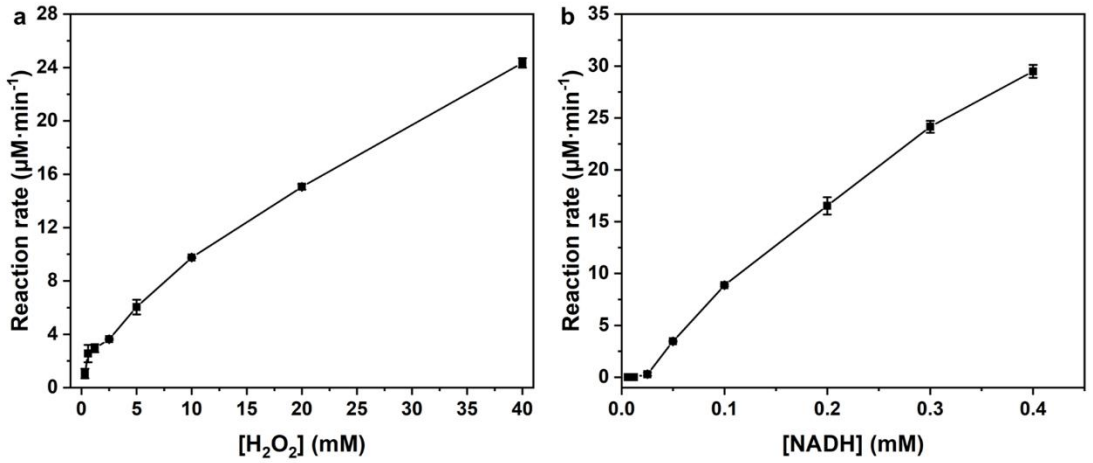

Figure S9. NADH (0.1 mM) oxidation reaction rates catalyzed by CuAsp in the presence of various concentrations of (a) H_2O_2 (0.3-40 mM) and (b) NADH (0.006-0.4 mM).

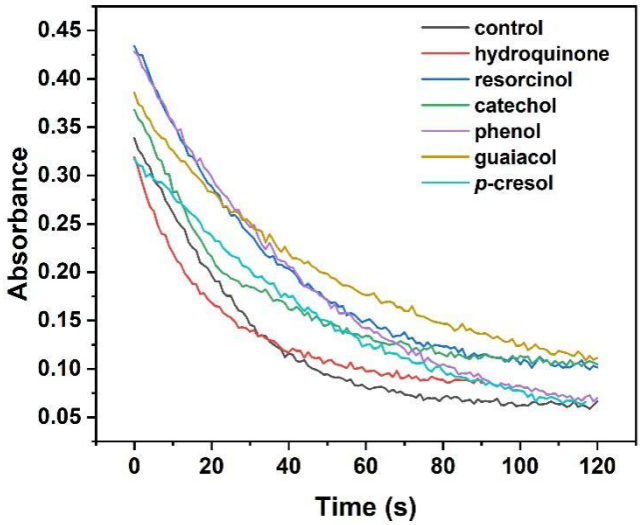

Figure S10. Time-dependent absorbance change at 340 nm of NADH oxidation reaction catalyzed by CuAsp in the presence of different mediators. Reaction conditions: 0.2 mM NADH, 50 mM H_2O_2, 0.125 mM CuAsp, 0.1 mM mediator, 1 mL of phosphate buffer (50 mM, pH8.0), room temperature.

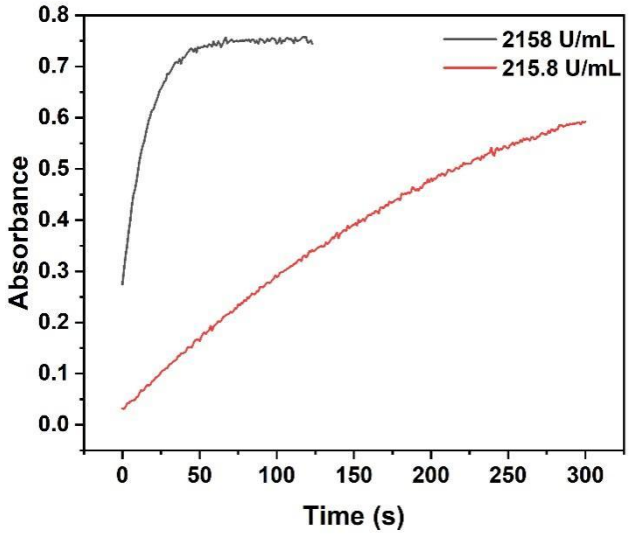

Figure S11. Time-dependent absorbance change at 340 nm of glucose oxidation reaction catalyzed by glucose dehydrogenase of different concentrations. Reaction conditions: 20 mM glucose, 0.2 mM NAD^+, 215.8/2158 U/mL glucose dehydrogenase, 1 mL of phosphate buffer (50 mM, pH8.0), room temperature.

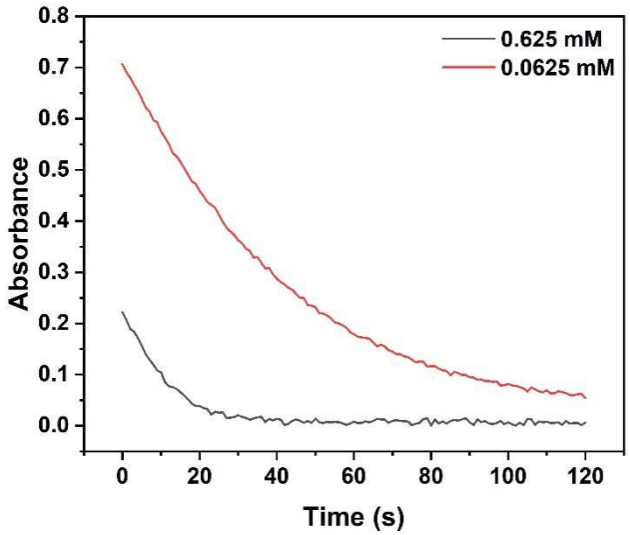

Figure S12. Time-dependent absorbance change at 340 nm of NADH oxidation reaction catalyzed by CuAsp of different concentrations. Reaction conditions: 0.2 mM NADH, 50 mM H_2O_2, 0.0625/0.625 mM CuAsp, 1 mL of phosphate buffer (50 mM, pH=8), room temperature.

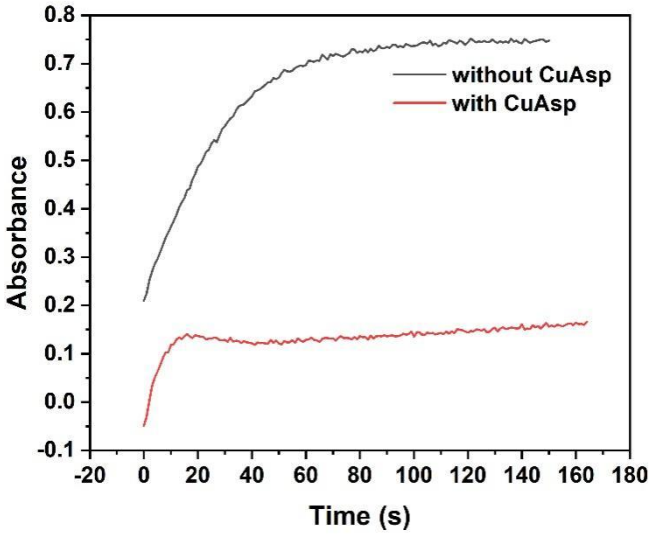

Figure S13. Time-dependent absorbance change at 340 nm of glucose oxidation reaction catalyzed by glucose dehydrogenase in the presence or absence of CuAsp. Reaction conditions: 20 mM glucose, 0.2 mM NAD^+, 2158 U/mL glucose dehydrogenase, 50 mM H_2O_2, 2 mL of phosphate buffer (50 mM, pH=8), room temperature.

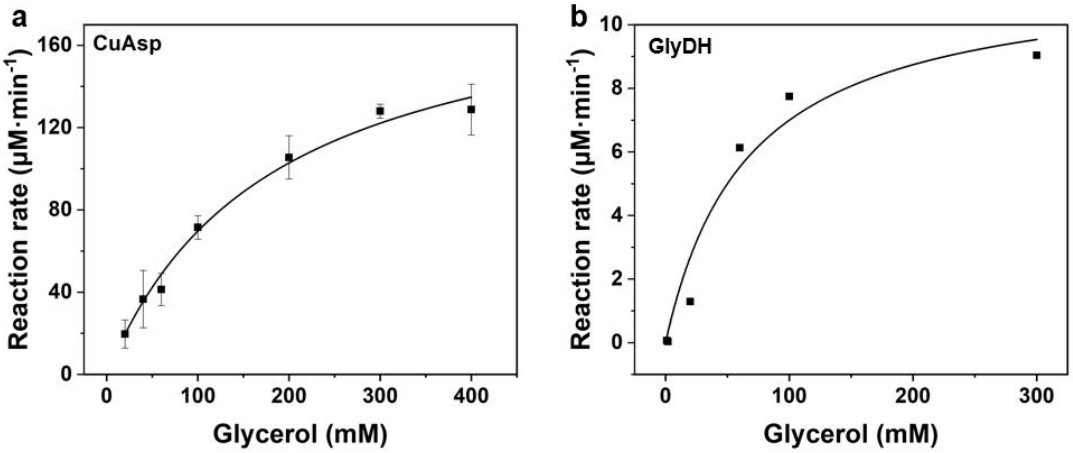

Figure S14. Glycerol oxidation reaction rates catalyzed by (a) CuAsp and (b) GlyDH in the presence of various concentrations of glycerol.

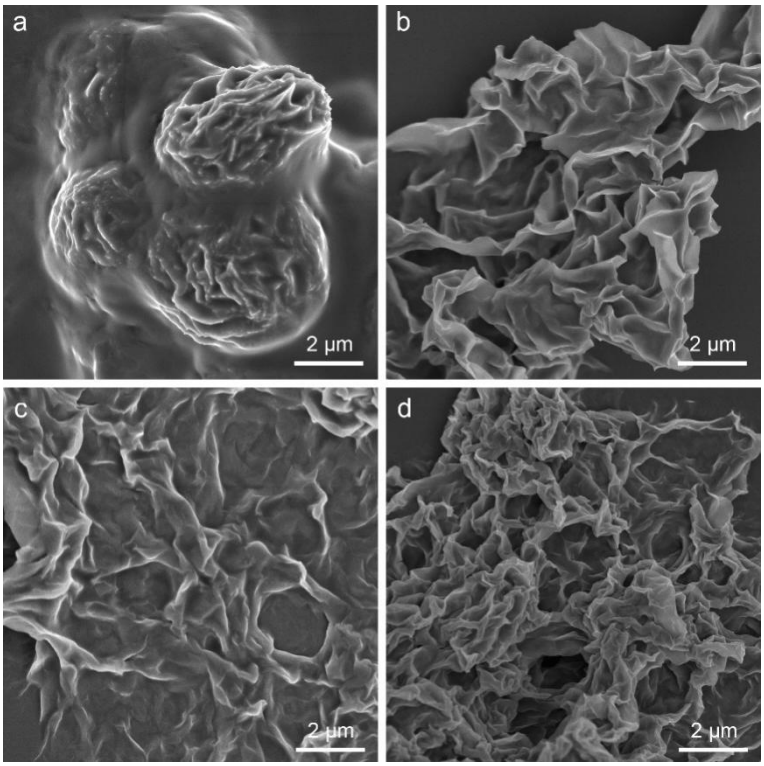

Figure S15. SEM images of CuAsp@GlyDH prepared after reaction for (a) 1 hour, (b) 4 hours, (c) 10 hours and (d) 24 hours.

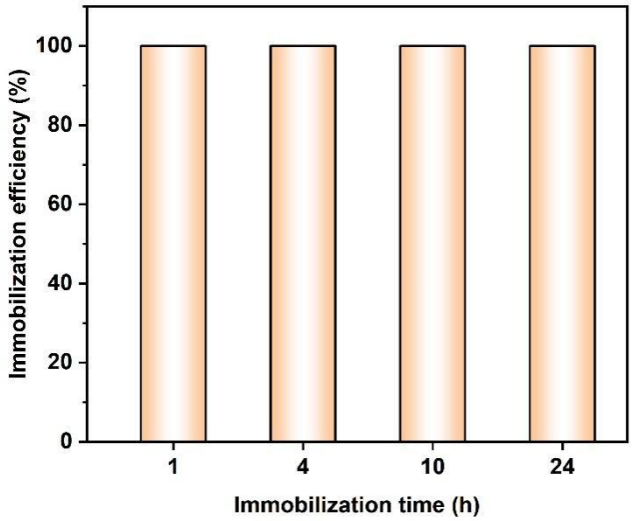

Figure S16. Immobilization efficiency of CuAsp@GlyDH with different immobilization time.

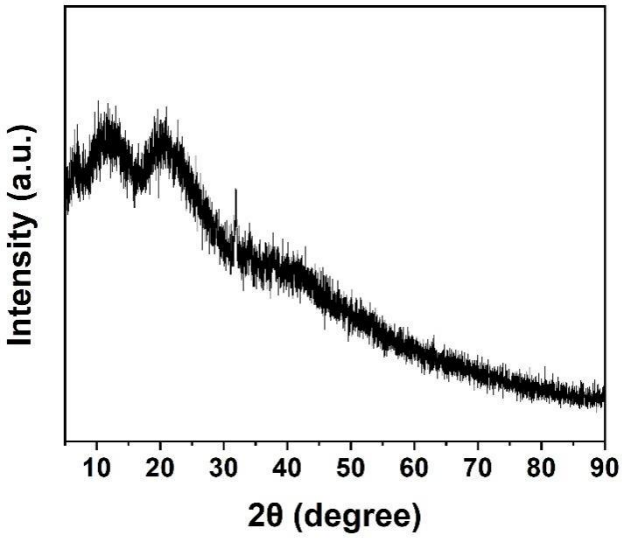

Figure S17. XRD pattern of CuAsp@GlyDH.

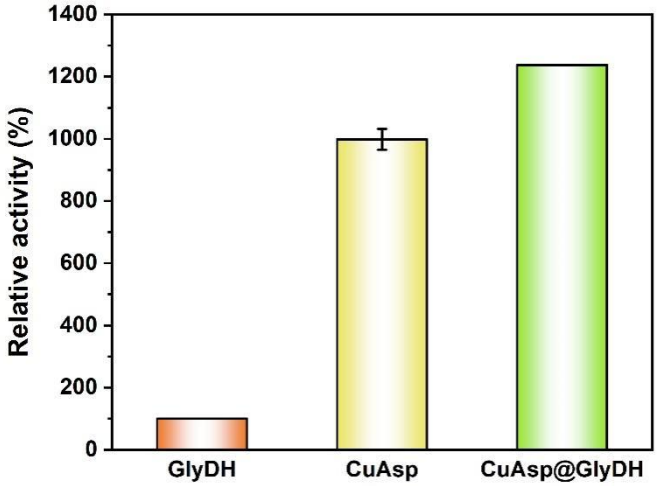

Figure S18. Relative activities of GlyDH, CuAsp and CuAsp@GlyDH.

Table S1. Results of inductively coupled plasma optical emission spectrometer (ICP-OES) detection and element analysis of CuAsp.

Element	N	C	H	Cu
Wt %	5.08	17.77	4.05	22.25

Table S2. Glucose dehydrogenase-catalyzed oxidation of glucose to gluconic acid.

Entry	Glucose (mM)	GDH (U/mL)	NAD^+ (mM)	H_2O_2 (mM)	CuAsp (mM)	Conversion (%)	TTN for cofactor
1	20	2158	0.2	0	0	0	0
2	20	2158	0.2	50	0	0	0
3	20	2158	0.2	50	0.625	47	47
4	20	2158	0.2	50	0.125	41	41
5	20	2158	0.02	50	0.625	50	498
6	20	2158	0.002	50	0.625	51	5100
7	50	2158	0.002	50	0.625	70	17500
8	50	21580	0.002	50	0.625	66	16393